CHINESE OPTICS LETTERS

Vol. 21, No. 5 | May 2023

Intracavity third-harmonic generation in a continuous-wave/self-mode-locked semiconductor disk laser

Chunling Li (李春玲)[1], Jia Cheng (成 佳)[1], Renjiang Zhu (朱仁江)[1], Tao Wang (王 涛)[1*], Lidan Jiang (蒋丽丹)[1], Cunzhu Tong (佟存柱)[2], Yanrong Song (宋晏蓉)[3], and Peng Zhang (张 鹏)[4**]

[1] College of Physics and Electronic Engineering, Chongqing Normal University, Chongqing 401331, China

[2] Changchun Institute of Optics, Fine Mechanics and Physics, Chinese Academy of Sciences, Changchun 130033, China

[3] Faculty of Sciences, Beijing University of Technology, Beijing 100124, China

[4] National Center for Applied Mathematics, Chongqing Normal University, Chongqing 401331, China

*Corresponding author: wangt@cqnu.edu.cn

**Corresponding author: zhangpeng2010@cqnu.edu.cn

Received December 9, 2022 | Accepted March 17, 2023 | Posted Online April 17, 2023

The high peak power of picosecond pulses produced by a self-mode-locked semiconductor disk laser can effectively improve the efficiency of nonlinear frequency conversion. This paper presents the intracavity frequency tripling in a self-mode-locked semiconductor disk laser, and a picosecond pulse train at 327 nm wavelength is achieved. The pulse repetition rate is 0.49 GHz, and the pulse width is 5.0 ps. The obtained maximum ultraviolet output power under mode locking is 30.5 mW, and the corresponding conversion efficiency is obviously larger than that of continuous-wave operation. These ultraviolet picosecond pulses have high spatial and temporal resolution and can be applied in some emerging fields.

Keywords: third-harmonic generation; self-mode locking; semiconductor disk laser; ultraviolet.

DOI: 10.3788/COL202321.051404

1. Introduction

Semiconductor disk lasers (SDLs), also known as vertical-external-cavity surface-emitting lasers, combine the advantages of both semiconductor surface-emitting lasers and solid-state disk lasers and can produce high power and good beam quality simultaneously[1–3]. Meanwhile, the emission wavelength of an SDL can be designed according to various practical needs; the external cavity can also be conveniently utilized for nonlinear frequency conversion or mode-locked operation.

Ultraviolet (UV) lasers have large single-photon energy as well as high spatial resolution and have many applications, including ion trapping[4], quantum information processing[5], laser cleaning[6], and UV spectroscopy[7]. A frequency-tripling-based UV continuous-wave (CW) SDL with 23 mW output power at 327 nm has been reported[8]. Through intracavity third-harmonic generation (THG) in an AlGaInP-based CW SDL, 78 μW output power and tunable emission wavelength from 224 to 226 nm have also been reported[9].

Typically, ultrashort laser pulses can be obtained by mode locking of an SDL using a semiconductor saturable absorber mirror (SESAM)[10]. However, a SESAM needs sophisticated wafer design and complicated epitaxial growth to meet the target parameters, including modulation depth, wavelength absorption, and saturation fluence[11,12], and this limits its application to a certain extent. Recently, a SESAM free mode-locked SDL, or self-mode-locked (SML) SDL has been demonstrated.

In the first publication of SML SDL, 2.35 W average output power with 778 fs pulse duration and 2.17 GHz repetition rate was performed[13]. Then, by the use of a six-mirror cavity, 930 fs pulse width, 210 MHz repetition rate, and 1.5 W average output power of SML SDL were obtained[14]. After that, an AlGaInP-based SML SDL at 666 nm wavelength was presented. The pulse width was 22 ps, and the repetition rate was 3.5 GHz[15].

In this paper, the THG under self-mode locking in an SDL was achieved for the first time, to the best of our knowledge. Compared with other methods of mode locking, self-mode locking needs no additional saturable absorbers such as SESAM and can make the laser more compact and stable. The produced UV picosecond pulses possess high spatial and temporal resolution simultaneously and are a potential candidate for many applications, e.g., fine micro-nanoprocessing, and the life sciences. In contrast, the UV CW laser or picosecond infrared laser is less competitive than the UV picosecond pulse to some extent. The high peak-power pulses generated by mode locking can significantly improve the efficiency of frequency tripling. The obtained maximum UV output power and the conversion efficiency of SML SDL are 30.5 mW and 0.092%, which are obviously larger than that of CW SDL, 11.7 mW and 0.072%.

2. Characteristic of Gain Chip

The epitaxial structure of the gain chip used in the experiment is shown in Fig. 1(a). Its growth sequence on a GaAs substrate is as follows: an AlGaAs etch stop layer, a GaAs cap layer, an AlGaAs window layer, InGaAs/GaAsP multiple quantum wells (MQWs), an AlGaAs/AlGaAs distributed Bragg reflector (DBR), and a GaAs protection layer. There are 12 InGaAs/GaAsP quantum wells in the active region, and the content of In in InGaAs is designed to meet the target laser wavelength of 980 nm. The designed center wavelength of the DBR is 980 nm.

In order to check whether the epitaxial quality meets our design, we measured the reflectivity spectrum of the DBR, the surface-emitting photoluminescence (PL) spectrum, and the laser spectrum; the results are shown in Fig. 1(b). The high reflectivity spectrum of a DBR ranges from 934 to 1016 nm at the center wavelength of 976 nm, the surface-emitting PL spectrum has two peaks near 922 and 966 nm, and the laser wavelength is about 980 nm. The PL spectrum was measured under low excitation (10 mW pump power), and the laser spectrum was measured under about 20 W pump power. It can be seen that the laser wavelength is about 14 nm larger than the peak value of the PL spectrum, and this difference is designed on purpose, since the peak wavelength of the PL spectrum will redshift at a rate of about 0.13 nm/°C as the temperature is increased. When the laser is under a higher pump, the increased temperature will push the PL spectrum to a longer wavelength, so as to meet the 980 nm target wavelength.

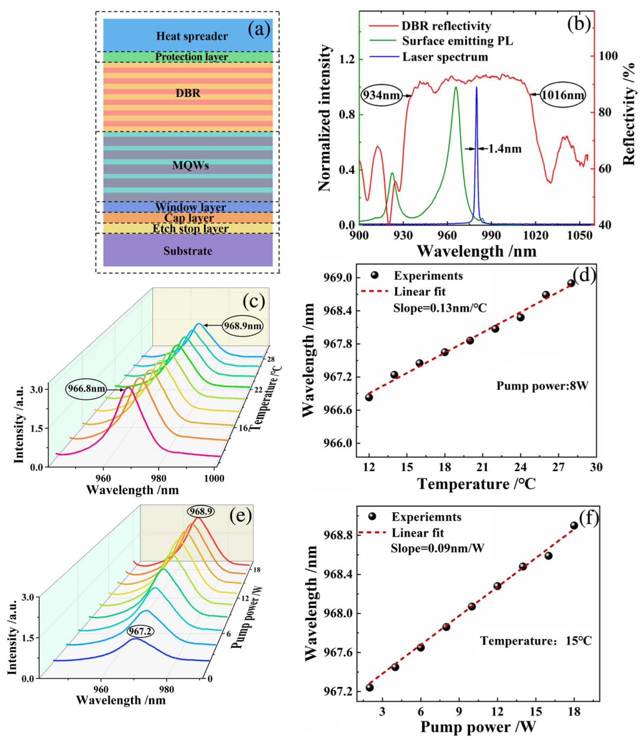

Fig. 1. (a) The epitaxial structure of the gain chip, (b) the DBR reflectivity, surface-emitting PL spectrum, and laser spectrum, (c) the surface-emitting PL spectra under various temperatures, (d) the peak wavelengths of surface-emitting PL spectra versus temperatures, (e) the surface-emitting PL spectra under various pump powers, and (f) the peak wavelengths of surface-emitting PL spectra versus pump powers.

Putting the fiber head of the spectrometer perpendicular to the surface of the gain chip and placing it at the front end of the chip, the collected spectrum is called a surface-emitting PL spectrum. Because it is the spontaneous emission spectrum of MQWs modulated by those epitaxial layers in the gain chip, the PL spectrum carries information of the epitaxial structure and can be roughly regarded as a cavity mode of the microcavity in the gain chip.

In view of the fact that the oscillating wavelength in an SDL essentially depends on the surface-emitting PL spectrum, we investigate the changes in the surface-emitting PL spectrum under different pump powers and various temperatures. The measured surface-emitting PL spectra with 8 W pump power and different temperatures are plotted in Fig. 1(c), and the relationship between its peak wavelengths and temperatures is described in Fig. 1(d). As can be seen from Fig. 1(d), the slope is 0.13 nm/°C, a little bit larger than the temperature coefficient (0.1 nm/°C) of a GaAs-based cavity mode.

We plot the measured surface-emitting PL spectra under 15°C temperature and various pump powers in Fig. 1(e), and its peak wavelengths versus pump powers are shown in Fig. 1(f). The slope in Fig. 1(f) is 0.09 nm/W. Considering the 0.09 nm/W together with the 0.13 nm/°C redshift in Fig. 1(d), it can be concluded that the temperature in the gain chip will be increased by about 0.69°C when the pump power is increased by 1 W. This means that the thermal effect of the gain chip needs to be further improved.

3. Experiments

The schematic and photograph of our practical experimental setup of the UV CW/SML SDL with a V-shaped cavity are shown in Figs. 2(a) and 2(b). An 808 nm fiber-coupled semiconductor laser with 60 W maximum output power is collimated and focused on the gain chip at an incident angle of about 30°. The diameter of the pump spot on gain chip is about

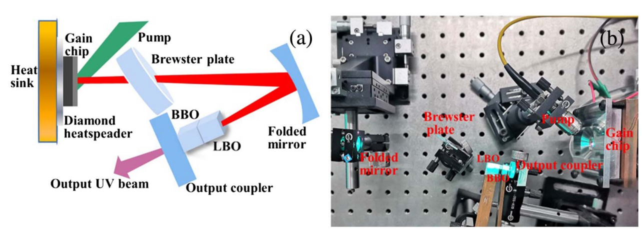

Fig. 2. (a) Schematic and (b) photograph of the experimental setup of the CW/SML UV SDL.

100 μm, approximately matched to the laser spot size. We use a plane–concave mirror with a 150 mm radius of curvature as the folded mirror, and it is high-reflectivity-coated at 980 and 327 nm and antireflectivity-coated at 490 nm. The output coupler (OC) is a flat mirror and is high-reflectivity-coated at 980 and 490 nm and antireflectivity-coated at 327 nm. To change the fundamental wave into a linearly polarized laser beam, so as to meet the phase-matching conditions in the second-harmonic generation and THG, a Brewster plate with 1 mm thickness is inserted into the cavity.

An LBO crystal is chosen as the nonlinear crystal for frequency doubling, and a BBO crystal is employed for the sum frequency. The 3 mm × 3 mm × 5 mm LBO crystal is cut for Type-I phase matching, and the 3 mm × 3 mm × 5 mm BBO crystal is cut for Type-II phase matching. Both sides of the LBO and BBO crystals are antireflectivity-coated at 980, 490, and 327 nm.

In the experiment, the length of the arm containing the Brewster plate is chosen to be about 183 mm, and the distance between the folded mirror and the OC is approximately 123 mm. To make the beam size of the laser on the nonlinear crystal as small as possible, so as to improve the efficiency of the nonlinear frequency conversion, the BBO crystal is put as close to the OC as possible, and the LBO crystal is placed next to it.

Figure 3 shows the UV output powers (measured by a photodiode power sensor with a 200–1100 nm wavelength range and a 50 mW power span) versus pump powers under 15°C temperature when the fundamental SDL is CW. The UV spectrum (measured by a spectrometer with a 200–800 nm wavelength range and 0.6 nm resolution) with a peak wavelength at 327 nm and full width at half-maximum (FWHM) of about 1.15 nm is also shown in the lower right corner. As can be seen, the threshold of the UV laser is 2.1 W. When the pump power reaches 16.6 W, the maximum output power is 11.7 mW, corresponding to a UV conversion efficiency of 0.070%, just the same as the previously reported work in Ref. [8].

The start of the self-mode locking in an SDL depends on an equivalent saturable absorber, which is formed by the Kerr lens in the active region of the gain chip and an aperture that could be either hard or soft. When the pump power is increased to a certain value, there will be noise pulses with sufficient strength in the cavity. The saturable absorber can select the pulse that meets the condition of saturation and gradually narrow its width. Finally, a balanced pulse circulating in the cavity is realized, and a stable output of the mode-locked pulse train is obtained.

After obtaining a CW SDL, by carefully adjusting the length of the resonator and appropriately reducing the pump spot, an SML SDL can be achieved without inserting any hard aperture. Figure 4 shows the autocorrelation trace (measured by an autocorrelator with a > 175 ps scan range and < 5 fs resolution) and the laser spectrum (measured by a spectrometer with a 780–1180 nm wavelength range and 0.18 nm resolution) [Fig. 4(a)], the mode-locked pulse train (recorded by an oscilloscope with a 10 GHz bandwidth and 50 GS/s sampling rate) [Fig. 4(b)], and the radio-frequency (RF) spectrum (detected by a spectrum analyzer with a 7.5 GHz bandwidth and 100 Hz–1 MHz resolution bandwidth) including the second-, third-, and fourth-harmonics of the SML SDL. It can be seen from Fig. 4(c) that the repetition rate of the stable SML pulses is 0.49 GHz (corresponding to the total cavity length of 306 mm). The Gaussian fit of the autocorrelation trace in Fig. 4(a) indicates a pulse width of about 5.0 ps. Considering the spectral bandwidth of 1.63 nm shown in the upper left corner, it can be concluded that the time bandwidth product of the SML pulse is 2.54, which is about 5 times the Fourier transform limit of a Gaussian pulse (0.441). This means that there is an obvious dispersion in the pulse, and we think that this dispersion may be caused by the nonlinear refractive index in the gain chip and the group velocity dispersion in the intracavity elements such as nonlinear crystals.

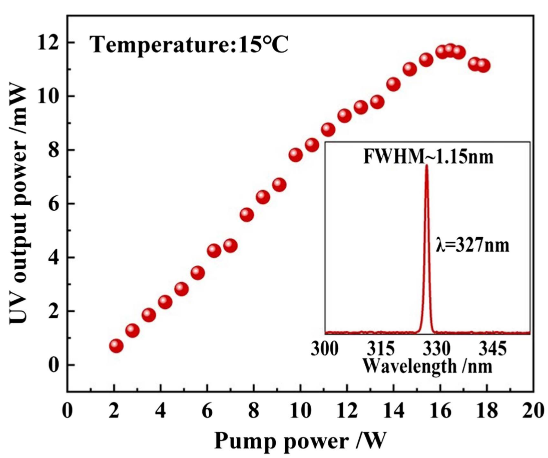

Fig. 3. The UV output powers of the CW SDL. The inset at the lower right corner is the spectrum of the UV laser.

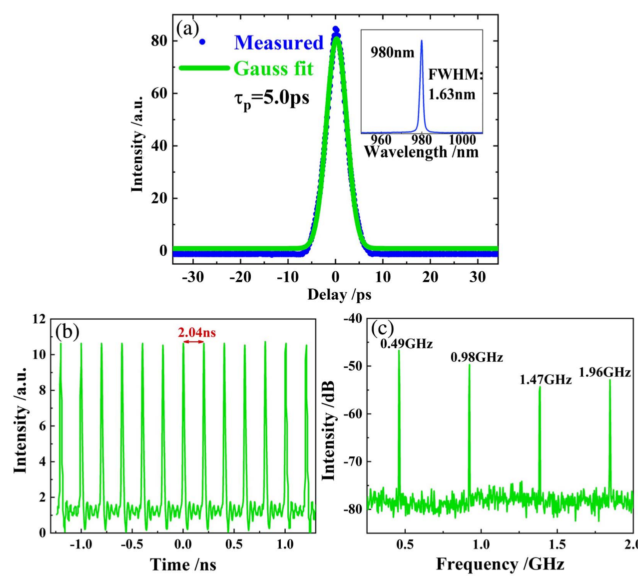

Fig. 4. (a) Autocorrelation trace, (b) the mode-locked pulse train, and (c) the RF spectrum, including the second-, third-, and fourth-harmonics of the SML SDL.

Limited by the spectral sensitivity of our photodetector (an 800–1700 nm wavelength range), the mode-locked pulse of 327 nm UV light cannot be directly measured. We detect the leaked 980 nm light at the back of the folded mirror, and ensure that the laser is in the mode-locked state through proper adjustment. This can indirectly justify that the UV light is also in the mode-locked state because although the nonlinear crystal will transform the frequency of the laser and change its temporal and spectral shape to a certain extent, the way of the pulsed operation of the laser will not be fundamentally changed. In other words, the mode-locking state will not be changed by the nonlinear crystal. The obtained SML UV output power from the very same cavity configuration and state is shown in Fig. 5. The measured beam quality M^2 factors of the fundamental wave and the spectrum of UV laser are also plotted at the upper left and lower right corners.

As can be seen from Fig. 5, the pump threshold of the SML UV laser is 2.8 W, and the maximum UV output power is 30.5 mW when the pump power is 33.0 W (corresponding to a UV conversion efficiency of 0.092%). Compared with the output of the CW UV in Fig. 3, both the maximum output power and the conversion efficiency of the SML UV SDL are obviously higher than that of CW UV SDL. We attribute this to two reasons: one is the high peak power of SML pulses (because it is conducive to enhance the conversion efficiency and output power of UV); the other is that the thermal effect of the laser may be alleviated partly under pulse operation, which also helps to increase the output power. The M^2 factors in the x and y directions are 1.03 and 1.00, respectively, thus showing good beam quality of the laser. The inserted Brewster plate in the resonator acts as a polarizer and a filter at the same time and can effectively fix the laser wavelength, so the output wavelength of the SML UV laser is relatively stable.

It can be seen from Figs. 1(b), 3, 4(a) and 5, that the FWHM widths of the CW and SML 980 nm lasers are 1.4 and 1.63 nm, and the FWHM widths of the CW and SML 327 nm UV lasers are 1.15 and 1.21 nm, respectively. For both the 980 nm infrared laser and the 327 nm UV laser, the spectrum of the SML light is wider than that of CW light. Because the spectra of the CW lasers are relatively wide, and the mode-locked pulses are of the magnitude of a picosecond, the above spectral broadening is not very obvious.

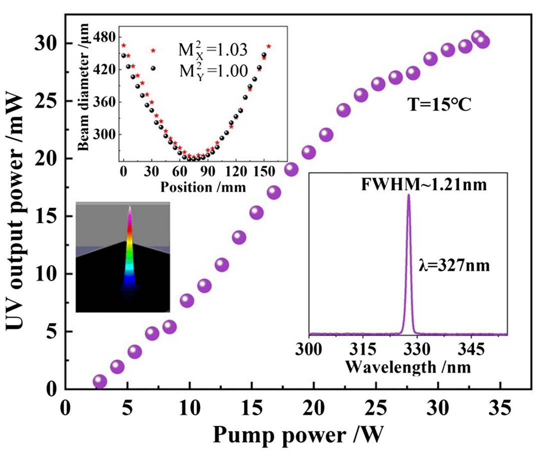

Fig. 5. UV output powers versus pump powers of the SML SDL. The insets at the upper left corner and lower right corner are the M^2 factors of beam quality and the UV spectrum.

4. Conclusion

In summary, we have demonstrated an intracavity THG in a CW/SML SDL. The wavelength of the obtained UV laser is 327 nm, and the maximum UV output powers of 11.7 mW under CW operation and 30.5 mW under mode locking are achieved. The SML SDL produces a stable pulse train with 5 ps duration and 0.49 GHz repetition rate. Compared with CW SDL, SML SDL produces not only higher maximum UV output power but also larger UV conversion efficiency. This is because of the high peak power of the mode-locked pulses.

Acknowledgement

This work was supported by the Cooperation Project between Chongqing Local Universities and Institutions of Chinese Academy of Sciences, Chongqing Municipal Education Commission (No. HZ2021007), the National Natural Science Foundation of China (Nos. 61904024, 61975003, 61790584, and 62025506), and the Science and Technology Research Program of Chongqing Municipal Education Commission (No. KJZD-M201900502).

References

1. M. Kuznetsov, F. Hakimi, R. Sprague, and A. Mooradian, “High-power (>0.5-W CW) diode-pumped vertical-external-cavity surface-emitting semiconductor lasers with circular TEM_{00} beams,” IEEE Photon. Tech. Lett. **9**, 1063 (1997).
2. B. Heinen, T. L. Wang, M. Sparenberg, A. Weber, B. Kunert, J. Hader, S. W. Koch, J. V. Moloney, M. Koch, and W. Stolz, “106 W continuous-wave output power from vertical-external-cavity surface-emitting laser,” Electron. Lett. **48**, 516 (2012).
3. M. Guina, A. Rantamäki, and A. Härkönen, “Optically pumped VECSELs: review of technology and progress,” J. Phys. D **50**, 383001 (2017).
4. R. C. Sterling, H. Rattanasonti, S. Weidt, K. Lake, P. Srinivasan, S. C. Webster, M. Kraft, and W. K. Hensinger, “Fabrication and operation of a two-dimensional ion-trap lattice on a high-voltage microchip,” Nat. Commun. **5**, 3637 (2014).
5. S. C. Burd, J. P. Penttinen, P. Y. Hou, H. M. Knaack, S. Ranta, M. Mäki, E. Kantola, M. Guina, D. H. Slichter, D. Leibfried, and A. C. Wilson, “VECSEL systems for quantum information processing with trapped beryllium ions,” arXiv:2003.09060 (2020).
6. B. Rauh, S. Kreling, M. Kolb, M. Geistbeck, S. Boujenfa, M. Suess, and K. Dilger, “UV-laser cleaning and surface characterization of an aerospace carbon fibre reinforced polymer,” Int. J. Adhes. Adhes. **82**, 50 (2018).
7. J. Paul, Y. Kaneda, T. L. Wang, C. Lytle, J. V. Moloney, and R. J. Jones, “Doppler-free spectroscopy of mercury at 253.7 nm using a high-power, frequency-quadrupled, optically pumped external-cavity semiconductor laser,” Opt. Lett. **36**, 61 (2011).
8. M. Polanik and J. Hirlinger-Alexander, “Generation of ultraviolet laser light by frequency tripling of a high-power infrared optically pumped

semiconductor disk laser," Annual Report (Institute of Optoelectronics, Ulm University, 2016), https://www.uni-ulm.de/fileadmin/website_uni_ulm/iui.inst.140/Jahresbericht/2016/UUlm-Opto-AR2016_MP.pdf.
9. J. M. Rodríguez-García, D. Pabœuf, and J. E. Hastie, "Tunable, CW laser emission at 225 nm via intracavity frequency tripling in a semiconductor disk laser," IEEE J. Sel. Top. Quantum Electron. **23**, 5100608 (2017).
10. E. J. Saarinen, R. Herda, and O. G. Okhotnikov, "Dynamics of pulse formation in mode-locked semiconductor disk lasers," J. Opt. Soc. Am. B **24**, 2784 (2007).
11. G. J. Spühler, K. J. Weingarten, R. Grange, L. Krainer, M. Haiml, V. Liverini, M. Golling, S. Schön, and U. Keller, "Semiconductor saturable absorber mirror structures with low saturation fluence," Appl. Phys. B **81**, 27 (2005).
12. A. A. Lagatsky, C. G. Leburn, C. T. A. Brown, W. Sibbett, S. A. Zolotovskaya, and E. U. Rafailov, "Ultrashort-pulse lasers passively mode locked by quantum-dot-based saturable absorbers," Prog. Quant. Electron. **34**, 1 (2010).
13. Y. F. Chen, Y. C. Lee, H. C. Liang, K. Y. Lin, K. W. Su, and K. F. Huang, "Femtosecond high-power spontaneous mode-locked operation in vertical-external cavity surface-emitting laser with gigahertz oscillation," Opt. Lett. **36**, 4581 (2011).
14. L. Kornaszewski, G. Maker, G. P. A. Malcolm, M. Butkus, E. U. Rafailov, and C. J. Hamilton, "SESAM-free mode-locked semiconductor disk laser," Laser Photonics Rev. **6**, L20 (2012).
15. R. Bek, M. Großmann, H. Kahle, M. Koch, A. Rahimi-Iman, M. Jetter, and P. Michler, "Self-mode-locked AlGaInP-VECSEL," Appl. Phys. Lett. **111**, 182105 (2017).